Det Kgl. Danske Videnskabernes Selskab.

Mathematisk-fysiske Meddelelser. **IV,** 7.

ON THE LICHTENBERG FIGURES

PART II.

1. THE DISTRIBUTION OF THE VELOCITY IN POSITIVE AND NEGATIVE FIGURES

2. THE USE OF LICHTENBERG FIGURES FOR THE MEASUREMENT OF VERY SHORT INTERVALS OF TIME

BY

P. O. PEDERSEN

WITH TWO PLATES

KØBENHAVN

HOVEDKOMMISSIONÆR: ANDR. FRED. HØST & SØN, KGL. HOF-BOGHANDEL

BIANCO LUNOS BOGTRYKKERI

1922

Introduction.

In Chapter IV of Lichtenberg Figures Part I[1] we have described a method for the measurement of the spreading-velocity of the positive and negative Lichtenberg figures, and the method was there used in determining the mean values of these velocities in the neighbourhood of the electrodes. In Chapter VII it was, furthermore, pointed out how a similar method may be used for the measurement of time-lag in electric sparks.

Since then we have carried out a rather lengthy investigation on this question, viz. time-lag in electric sparks, the results of which will be published elsewhere. In the course of this investigation it was found desirable to investigate how the spreading-velocity varies from the electrode, where the velocity is greatest, to the final boundary of the figure, where it is zero. It was also found necessary to make a closer study of the theory of these measurements and especially to investigate the possible errors introduced by sloping wave fronts. The results of our investigation of these two questions are presented in the present paper.

The main problem to be solved may be stated as follows: A Lichtenberg figure starts at a certain moment from

[1] P. O. PEDERSEN: On the Lichtenberg Figures Part I. Vidensk. Selsk. Math.-fysiske Medd. I, 11. Copenhagen 1919. In the following referred to as L. F. I.

an electrode and t seconds later its outer boundary has reached to a distance of r cm from the electrode. The described space r will then depend upon the time t, say

$$r = F(t). \tag{I}$$

The function F depends upon the amplitude of the impulse, the nature and density of the gas, the thickness of the photographic plate (P in Fig. 1), and possibly other conditions. The problem is to determine the function F.

This function being known, the velocity U, is given by

$$U = \frac{dF(t)}{dt} = U(t), \tag{II}$$

and the time-interval t corresponding to a known space r may be found by solving (I) with regard to t. We will write this solution in the form

$$t = f(r). \tag{III}$$

On the other hand if (II) or (III) are known we may therefrom deduct the relation (I).

The final range R of the figure will be given by

$$R = F(\infty). \tag{IV}$$

We have determined the relation (I) in two different ways:

a) By measurements of corresponding values of t and r by means of the method given in L. F. I. and briefly described in section 1. below.

b) By deducing the relation (II) mathematically from the shape of the separating line between two figures originating from straight electrodes. The details of this method are given in section 2. below.

In section 3. it is proved that the results obtained by means of a) and b) agree with each other.

Section 4. treats of the influence of sloping wave fronts, section 5. discusses some details with regard to the shape of the separating line, and section 6. contains some concluding remarks.

1. The Method used for the Measurement of Corresponding Values of the Time t and Space r in Relation (I).

The method used for these measurements is indicated in Fig. 1. E is a small influence machine, connected to the

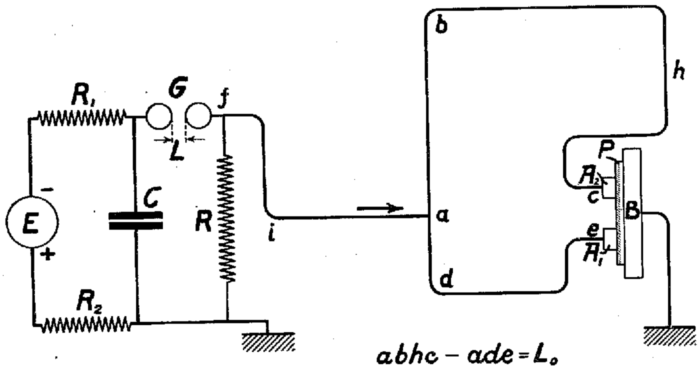

Fig. 1. Diagram of Circuit used for the Measurement of Corresponding Values of t and r in Formula (I).

condenser C through two large resistances R_1 and R_2, f. inst. two slate pencils. G is the primary spark gap, A_1 and A_2 two electrodes, the shape and relative position of which are shown in Fig. 2. A_1 and A_2 are placed on the sensitive film of a photographic plate P, resting on a metal plate B connected to earth. A wire $f\,i\,a$ connects the primary spark gap with the point a of the loop $e\,d\,a\,b\,h\,c$ connecting A_1 and A_2, and the length of the wire $a\,b\,h\,c$ is L_0 meters longer than $a\,d\,e$. One terminal of the condenser

C is connected directly to earth, the wire system and the electrodes A_1 and A_2 through the large resistance R.

In order to make a measurement the handle of the influence machine is slowly turned until a spark passes the spark gap G. An electric impulse or wave will then

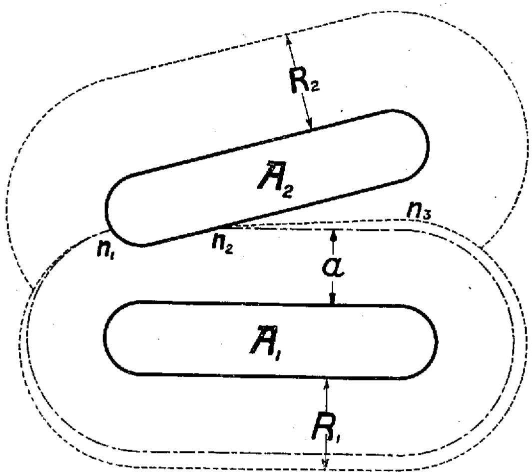

Fig. 2. Shape and Relative Position of the Lichtenberg Electrodes A_1 an A_2 in Fig. 1.

travel out along the wire $f\,i\,a$, and at the point a this impulse is partly reflected and partly transmitted into the wires $a\,b$ and $a\,d$. The reflected wave is travelling back along the wire $a\,i\,f$, and the two transmitted waves travel respectively along the wires $a\,b\,h\,c$ and $a\,d\,e$. If the impulse impedances of the three wires meeting in the point a are equal, the amplitude of the reflected impulse will be $-\frac{1}{3}V_0$, while that of the transmitted impulses will be $\frac{2}{3}V_0$, the amplitude of the incident impulse being denoted by V_0.

Of the two transmitted impulses that one travelling along the wire $a\,d\,e$ will reach the electrode A_1 t_0 seconds before the impulse travelling along $a\,b\,h\,c$ reaches the electrode A_2, where

$$t_0 = \frac{L_0}{v} = \frac{L_0}{3 \times 10^8}, \tag{a}$$

the wire $a\,b\,h\,c$ being L_0 meters longer than $a\,d\,e$. It is supposed that the impulses travel with a velocity v equal to that of light. In reality the velocity will be a little smaller, and t_0 determined by means of (a) therefore comes out too small; but if the wires are not too close to other conductors this error will only be relatively unimportant.

The Lichtenberg figure originating from A_1 will therefore start t_0 seconds before a corresponding figure starts from A_2. The first figure has therefore spread over a space a (see Fig. 2) before a figure starts from A_2. The two figures will meet along a line $n_2 n_3$, the separating line, of which it is proved later on, that that part which is situated between the straight edges of the electrodes A_1 and A_2 generally is also very nearly a straight line. This straight part of the separating line starts from the point n_2 on the edge of A_2, and the distance from n_2 to the edge of A_1 is equal to the distance a travelled by the figure from A_1 in t_0 seconds. In this way corresponding values of the two variables in formula (I) are determined.

2. Impulses with Extremely Steep Front, Shape and Position of Separating Line.

We shall now consider how the position and shape of the separating line depends upon the function U in formula (II). In order to simplify our consideration we suppose, for the present, that the fronts of the impulses arriving at the electrodes A_1 and A_2 are extremely steep. We may then indicate the velocities of the figures spreading from A_1 and A_2 by means of the curves $U_1(t)$ and $U_2(t)$ shown in Fig. 3, I. The velocity U_1 starts at the time $t = 0$

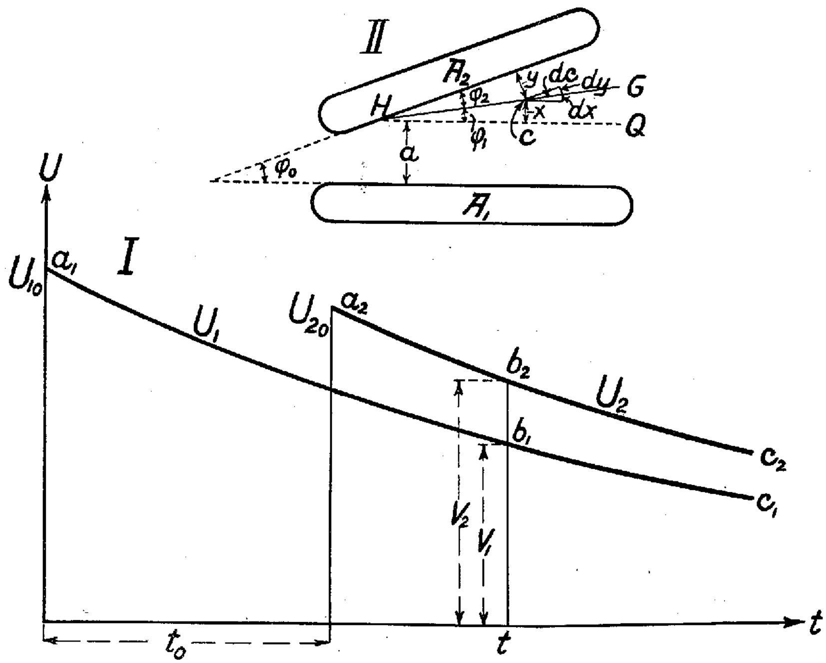

Fig. 3. Part I: Velocity Curves U_1 and U_2 for Figures spreading from respectively A_1 and A_2, the Figure from A_1 starting t_0 seconds before that from A_2.
Part II: Position of the Electrodes A_1 and A_2 and of the Straight Part HG of the Separating Line.

with the initial velocity U_{10}, and U_2 at the time $t = t_0$ with the velocity U_{20}.

At the moment the figure starts from A_2 the outer boundary of the figure from A_1 will be at a distance a from the edge of A_1, where

$$a = \int_0^{t_0} U_1 \cdot dt. \tag{1}$$

The separating line starts at the point H on the edge of

A_2 just reached by the figure from A_1 at the moment the figure from A_2 starts (see Fig. 3, II). The distance of H from the edge of A_1 is therefore equal to a.

Later on it will be proved that that part HG of the separating line which is lying between the straight edges of A_1 and A_2 is also a straight line for all values of the time interval t_0.

We shall now consider the mathematical consequences of this straightness of the separating line with regard to the possible forms of the velocity function U.

Let dc be an element of the straight separating line (see Fig. 3, II), we have then with the symbols used in the figure:

$$dx = dc \cdot \sin \varphi_1, \quad \text{and} \quad dy = dc \cdot \sin \varphi_2 .$$

At the same time we have

$$dx = U_1 \cdot dt, \quad \text{and} \quad dy = U_2 \cdot dt,$$

dt being the time it takes to form the element dc of the separating line while U_1 and U_2 are the instantaneous values of the two velocities at the moment t.

We have accordingly

$$\frac{dy}{dx} = \frac{\sin \varphi_2}{\sin \varphi_1} = \frac{U_2}{U_1} = k, \tag{2}$$

were k is a constant.

Equation (2) may be written

$$U_2(t) = k \cdot U_1(t). \tag{3}$$

If, instead of the time interval t_0 we choose $t_0 + dt$, the separating line will also be straight, but the corresponding constant k will have a different value k' dependent upon dt but independent of t. We may therefore write

$$k' = k(1 + \alpha\, dt),$$

were α is a constant.

Instead of (3) we get

$$U_2(t-dt) = k' \cdot U_1(t). \tag{4}$$

From (3) and (4) it is easily deduced that

$$\frac{d\,U_2}{U_2} = -\alpha \cdot dt,$$

or

$$U_2(t) = U_2' \cdot e^{-\alpha t} = U_{20} \cdot e^{-\alpha(t-t_0)}, \tag{5$_1$}$$

and therefore

$$U_1(t) = U_{10} \cdot e^{-\alpha t}, \tag{5$_2$}$$

the value of the constant k being

$$k = \frac{U_{20}}{U_{10}} \cdot e^{\alpha t_0}. \tag{5'}$$

When the separating line is straight, the velocity functions must necessarily be those given in (5_1) and (5_2) in which U_{10}, U_{20}, and α are constants. And vice versa with these velocity functions the part of the separating line under consideration will always be straight.

It follows from equation (5_2) that

$$r = F(t) = \int_0^t U_1 \cdot dt = \frac{1}{\alpha} \cdot U_{10} \cdot (1-e^{-\alpha t}), \tag{6}$$

and the range

$$R_1 = \frac{1}{\alpha} U_{10}, \tag{7}$$

or

$$U_{10} = \alpha R_1. \tag{7'}$$

Equations (6) and (5_2) may therefore be written:

$$r = F(t) = R_1(1-e^{-\alpha t}), \tag{8}$$

and

$$U_1 = \alpha(R_1 - r) = U_{10} - \alpha r. \tag{9}$$

The velocity decreases linearly with increasing distance from the edge of the electrode.

We shall next determine how the angle φ_2 between the separating line and the electrode A_2 depends upon the ratio of the velocities and on the angle $\varphi_0 = \varphi_1 + \varphi_2$ between A_1 and A_2.

We evidently have (see Fig. 3, II):

$$\frac{\sin \varphi_2}{\sin \varphi_1} = \frac{U_2(t)}{U_1(t)} = \frac{U_{20}}{U_{10}} \cdot e^{\alpha t_0} = \frac{U_{20}}{U_{10}} \cdot \frac{R_1}{R_1 - a} = c \cdot \frac{R_1}{R_1 - a}, \quad (10)$$

where $c = \frac{U_{20}}{U_{10}}$ is the ratio between the velocities just at the edges of the electrodes, and a is the distance travelled in t_0 seconds by the figure originating from A_1.

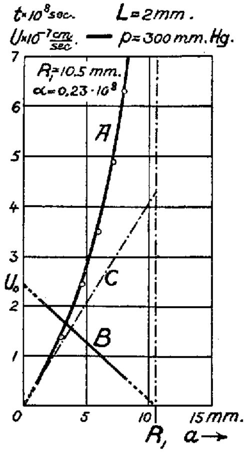

Fig. 4. Negative Figures. $L = 2$ mm; Pressure $p = 300$ mm Hg. $R_1 = 10.5$ mm; $\alpha = 0.23 \times 10^8$.

Supposing the angles φ_1 and φ_2 are so small that in formula (10), without any serious error, we may substitute φ_1 and φ_2 for respectively $\sin \varphi_1$ and $\sin \varphi_2$, this formula is then reduced to

$$\varphi_2 - \varphi_1 = \Delta\varphi = \varphi_0 \frac{a - (1-c) R_1}{(1+c) R_1 - a}. \quad (10_1)$$

The angle φ_2 is then given by

$$\varphi_2 = \tfrac{1}{2} (\varphi_0 + \Delta \varphi). \quad (11)$$

If $U_{10} = U_{20}$, $(c=1)$, equation (10_1) reduces to

$$\Delta \varphi = \varphi_0 \frac{a}{2R_1 - a}. \quad (10_2)$$

In the following the formulae (11) and (10_1) or (10_2) are used for the calculation of the angle between the separating line and A_2.

3. Experimental Proof by Means of the Method described in Sect. 1 of the Velocity Functions deduced in Sect. 2.

In Figs. 4—6 the points indicated by small circles represent corresponding values of a and t_0 determined by the method described in sect. 1, while the curves marked

A represent the theoretical relationship between a and t_0 according to equation (8), viz.:

$$a = R_1 (1 - e^{-\alpha t_0}).$$

The value of R_1 is measured directly on the photographic plate, while for α we have chosen such a value that the experimental points fall as closely as possible to the curve A.

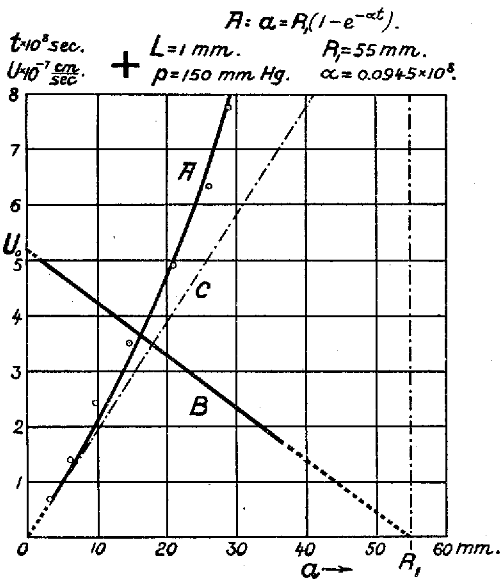

Fig. 5. Positive Figures: $L = 1$ mm; $p = 150$ mm. Hg.; $R_1 = 55$ mm; $\alpha = 0.0445 \times 10^8$.

Taking into account that there is only one arbitrary constant, namely α, the value of which can be chosen so as to accommodate the theoretical and the experimental values as much as possible, we may say that the results obtained by the two methods agree very well with each other.

In Figs. 4—6 the straight lines B represent the spreading-velocity of the figures at different distances from the electrodes according to formula (9). The equation of those lines is therefore

$$U_1 = \alpha (R_1 - a) = U_{10} - \alpha a. \qquad (9')$$

The broken lines C represent the tangents to the A-curves at the origin.

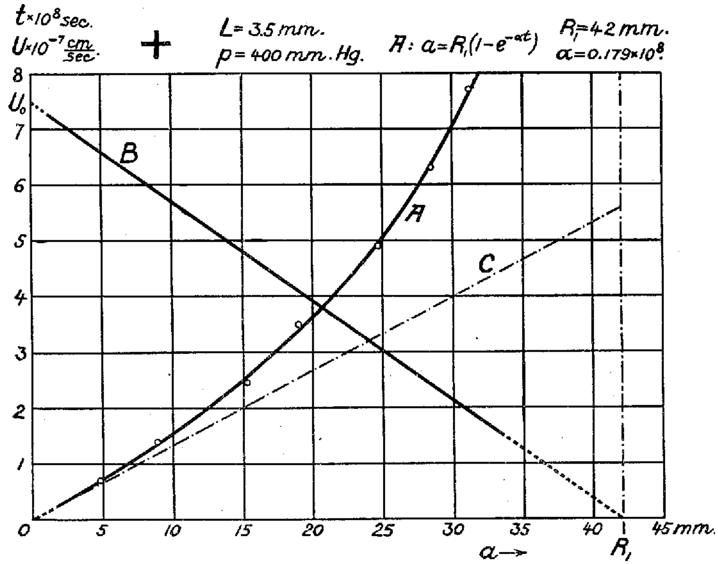

Fig. 6. Positive Figures. $L = 3.5$ mm; $p = 400$ mm Hg.; $R_1 = 42$ mm; $\alpha = 0.179 \times 10^8$.

In Fig. 7 the curve D represents the velocity function corresponding to the A-curve in Fig. 5.

The outermost parts of the velocity lines B in Figs. 4—6 and D in Fig. 7 are shown in broken lines and are only to be considered as theoretical extrapolations. It is hardly probable that the velocity goes down quite to zero, but the reduction in the range caused hereby is probably small.

Besides the experiments, of which the results are given in Fig. 4—6, we have made a number of other investigations aiming at the determination of the dependence of α upon spark length, gas pressure etc.

The results of these investigations are shown in Figs. 8 and 9 for positive and negative figures respectively. The values of α seem in both cases to be rather independent of the spark length but to increase linearly with increasing pressure of the gas and much more rapidly for positive than for negative figures. In both cases the value of α seems to converge towards a definite value — about 0.075 $\times 10^8$ for positive and 0.15×10^8 for negative figures — when $p \to 0$.

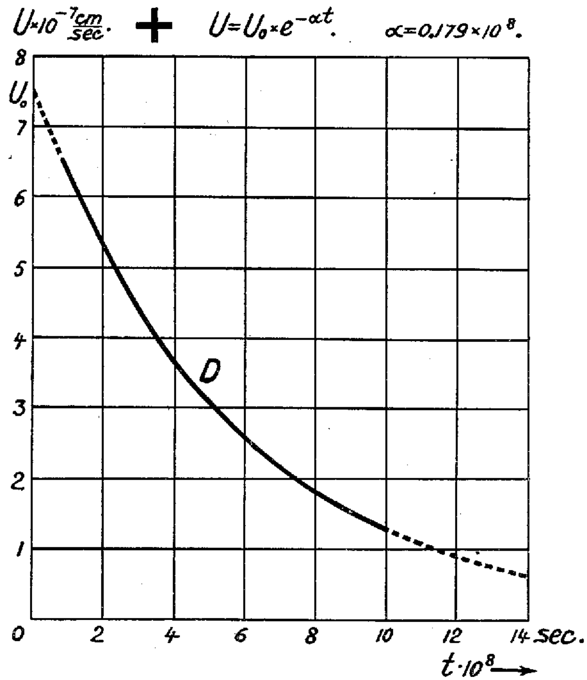

Fig. 7. Theoretical Velocity Curve corresponding to Curve A in Fig. 5.

In the upper parts of Figs. 8 and 9 are also shown the corresponding values of the range R and the initial velocity V_0. In most cases the ratio between gas pressure and spark length (both in mms.) has been equal to 100. Where this is not the case a number at the experimental point gives the value of that ratio. The curves marked R and U_0 give — for the said ratio equal to 100 — an approximate representation of the range and the velocity as depending upon the pressure of the gas.

According to the evidence given on the preceding pages

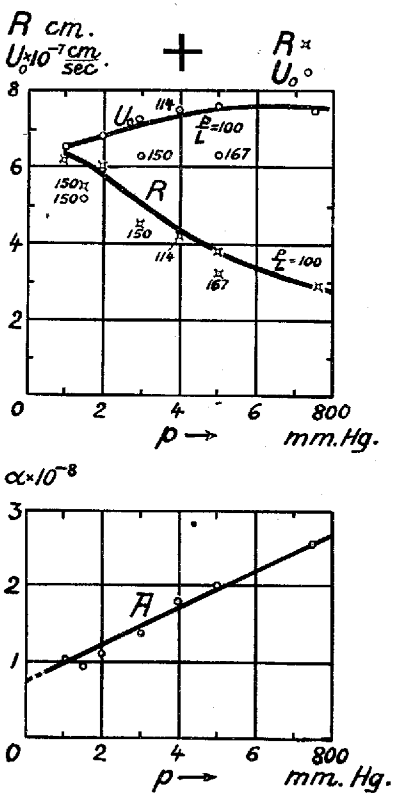

Fig. 8. Positive Figures. The values of the Coefficient α, the Range R and the initial Velocity V_0 as dependent upon the Pressure p and Spark Length L.

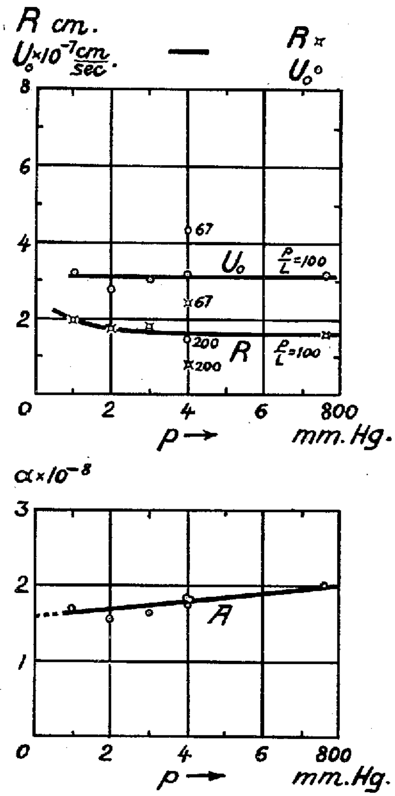

Fig. 9. Negative Figures. [In the lower parts of Figs. 8 and 9 the Ordinates are $\alpha \cdot 10^{-9}$ and not $\alpha \cdot 10^{-8}$ as indicated in the Figures.]

there can be but little doubt that our solution — represented by the equations (5_2), (8) and (9) — of the problem treated of is substantially correct.

In what follows we shall treat of some possible sources of errors and their elimination, investigate in some detail the general shape of the separating line and last but not least furnish some experimental evidence of the straightness of the often mentioned part of this line.

Before closing this section it is necessary, however, to make a single remark. The spreading-velocity of the Lichtenberg figures, with which we are dealing here, are by no means the same as the velocities, by which the "sliding sparks" (Gleitfunken) studied by M. Toepler[1] extend themselves. It will be shown elsewhere that the two phenomenae, Lichtenberg figures and sliding sparks, differ very much from each other. Toepler found — by making use of the velocity of sound waves — that the velocity of a sliding spark is practically constant almost to the end of the spark, and there is hardly any reason to doubt the correctness hereof.

4. The Influence of Sloping Wave Fronts on the Shape of the Separating Line.

We have until now supposed that the wave fronts of the impulses were extremely steep in which case the initial velocity at the edge of the electrodes is also the maximum velocity. Generally, however, the wave fronts are more or less sloping, increasing gradually from zero to the maximum amplitude of the impulse. The velocity will then also increase gradually up to its maximum value U_0' (see Fig. 10 Part III). The duration of the sloping front is in Fig. 10 Part II—IV taken to be equal to τ_0. The amplitude of the impulse is taken as constant for all values of t greater than τ_0 (see Fig. 10 Part II) and for the same values of t the velocity is supposed to decrease exponentially with t.

[1] M. Toepler: Ann. d. Phys. (4) 21, p. 193—222, 1906.

We now extend this exponential velocity curve backwards to the point d_1, which is chosen in such a way that the two shaded areas, $o_1 e_1 b_1$ and $b_1 d_1 c_1$ are equal. The velocity corresponding to the point point d_1 is denoted by U_0 and

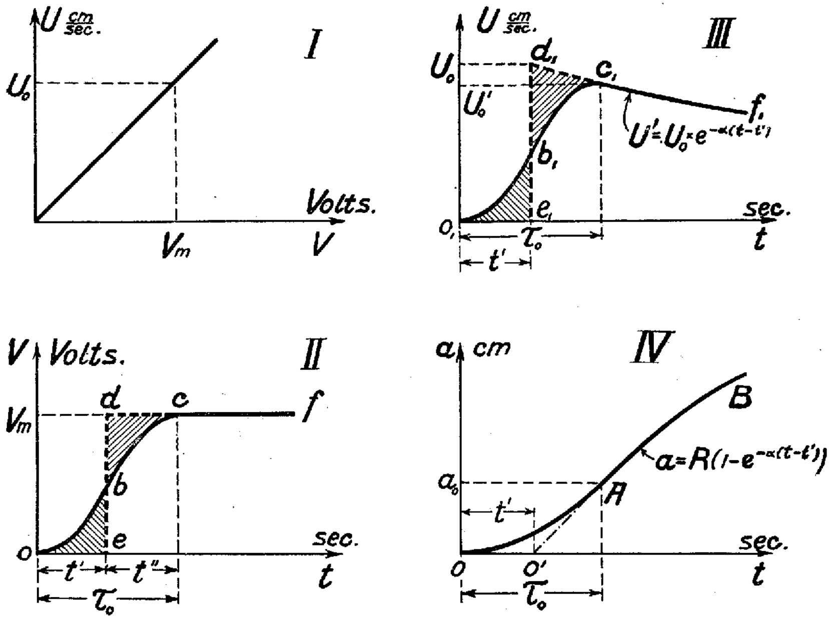

Fig. 10. The straight Line in Part I represents a Linear Relationship between the Velocity at the Edge of the Electrode and the Voltage of same.

In Part II the Line $o\,b\,c\,f$ represents the Front of an Impulse. The curve $o_1 b_1 c_1 f_1$ in Parts III represents the Corresponding Velocities.

The curve *OAB* in Part IV represents the Distance travelled by the Outer boundary of the Figure in the Time t.

we call the curve $d_1 c_1 f_1$ the equivalent velocity curve, the equation of which is

$$U' = U_0 \cdot e^{-\alpha(t-t')} \qquad [U' = 0 \text{ when } t < t']. \qquad \text{(b)}$$

The distance a which the outer boundary has reached in the time t is given by

$$a = \int_0^{t_0} U \cdot dt\,, \qquad \text{(c)}$$

and for all values of t_0 greater than τ_0 we may in this formula substitute the equivalent velocity U' for the actual velocity U.

In Fig. 11 we have shown two identical velocity curves U_1 and U_2 with a time interval of t_0 seconds and the corresponding distances r_1 and r_2 travelled by the figures from A_1 and A_2. It will presently be shown that what is measured on the photographic plate is the time interval

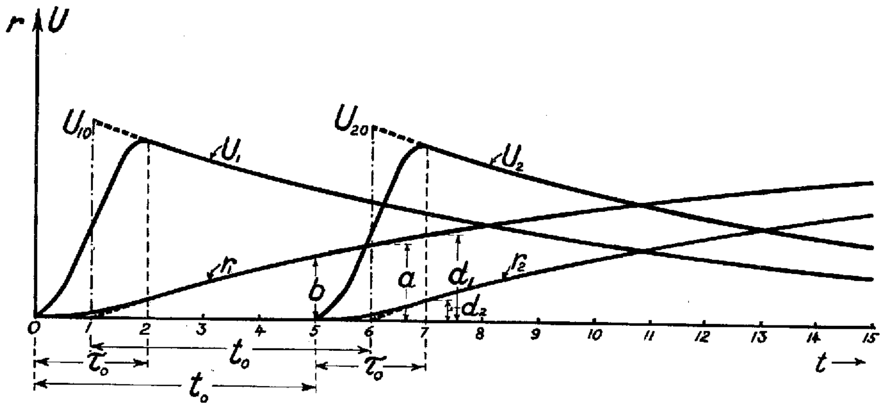

Fig. 11. Two identical Velocity Curves U_1 and U_2 with a Time Interval of t_0 and the Corresponding Distance Curves r_1 and r_2.

between the steep fronts of the equivalent velocity curves. What really is desired is to know the interval between the fronts of the two corresponding electrical impulses. In so far as the two impulses are identical in shape the time interval between the impulses will be exactly equal to the interval between the steep fronts of the equivalent velocity curves. If the two impulses have differently shaped fronts it is perhaps a little doubtful how to define the time interval between them. In this case the most natural way to define this time interval will presumably be the following: The front of the voltage impulse $obcf$ (see Fig. 10 Part II) is transformed to the "equivalent" voltage curve with vertical front, $ebdcf$, where the position of the vertical front ed is chosen in such a way that the two areas oeb and bdc are equal. The time interval between the two voltage impulses is then taken as the interval between the vertical fronts of the two equivalent voltage impulses. If, as indicated in Fig. 10 Part I, the velocity U is proportional to the voltage V, the time interval between the vertical fronts of the equivalent velocity curves is very nearly equal to the time interval between the vertical fronts of the equivalent voltage impulses. Even in the cases where there is no proportionality between U and V the two time intervals will very nearly be equal. We may, therefore, without serious errors take the time interval between two voltage impulses as the time interval between the vertical fronts of the equivalent velocity curves, and this last interval is, as will be shown shortly, equal to the t_0 measured on the photographic plate. In all cases where the wave fronts of the two impulses are identical in form the error is zero.

In order to illustrate the influence of sloping wave fronts we have in Fig. 12 shown the separating line which would result from the two velocity curves shown in Fig. 11 and with a time interval of $t_0 = 5$. If the wave fronts were vertical the straight part ed of the separating line would be continued to the point c at the edge of A_2. The sloping of the wave fronts causes the part dc of the separating line to bend down to the position db_2. The distance of the point b_2 from the edge of A_1 is equal to the distance b travelled by the figure from A_1 at the moment when the figure from A_2 just begins to start (see Fig. 11). The separating line again starts from the edge of A_2

at the point b_1 where the distance from A_1 again is equal to b. From the last point the separating line goes in a bent curve to the point g.

It is very easy by means of the r_1- and r_2-curves of Fig. 11 to draw the separating line in Fig. 12 and corresponding distances are marked in the same way in these

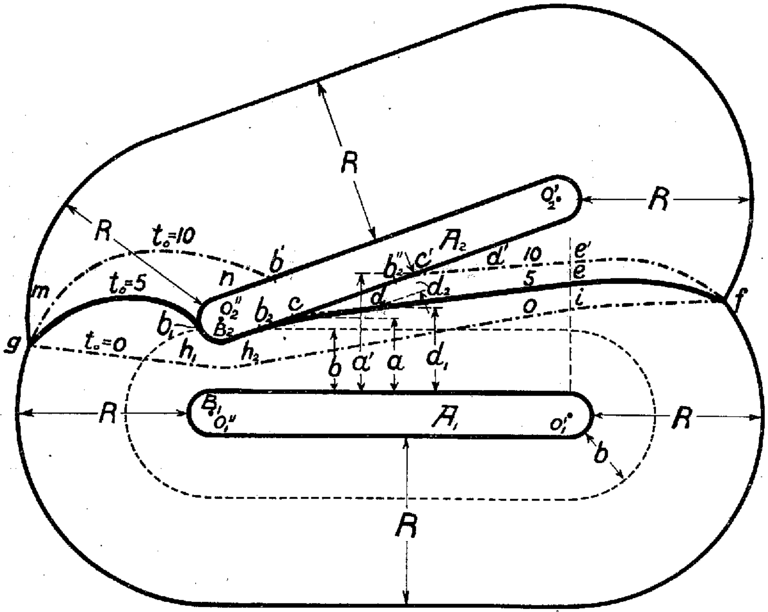

Fig. 12. Two Separating Lines corresponding to the Sloping Wave Fronts of Fig. 11. One for $t_0 = 5$ shown with a Heavy Line, the other, corresponding to $t_0 = 10$, in a broken Line. The final Range R is the same in both Figures.

two figures. Between the points d and e the separating line according to section 2., is a straight line, and, if extended beyond d, this straight line cuts the edge of A_2 in a point c. It is easily seen from Fig. 11 that the distance a of this point c from the edge of A_1 is equal to the distance travelled by the figure from A_1 at the moment, the figure would start from A_2 if the velocity curve was the equivalent one with vertical front. The distance a is therefore equal to the distance travelled in the time t_0 by a figure spreading out according to the equivalent velocity curve. Such distances a it is which are plotted against the corresponding values of t_0 in Figs. 4—6.

5. The General Shape of the Separating Line. Experimental Proof of the Straightness of Part of this Line.

In Fig. 12 we have — besides the separating line already mentioned — in broken lines shown two other lines based on the velocity curves of Fig. 11 and corresponding to respectively $t_0 = 0$ and $t_0 = 10$. The common ends of all these separating lines will be at the points g and f. For $t_0 = 0$ the outer ends $g h_1$ and $i f$ of the separating line are straight lines passing vertically through the middle points of the two center lines $o'_1 o'_2$ and $o''_1 o''_2$. The part $h_2 i$ of this separating line is also a straight line, namely the bisector of the angle between the edges of A_1 and A_2. For $t_0 = 10$ the straight part of the separating line is $e' d'$, while a' is the distance travelled by the outer boundary of the figure from A_1 in the time $t_0 = 10$.

In order to compare the theoretical with the actual separating line we have in Figs. 13, and 16—18 reproduced two positive and two negative velocity figures with the theoretical separating lines indicated by broken lines. We shall later on discuss the agreement between the actual and the theoretical separating lines. It is necessary to point out, however, that for such lines as the one shown in Fig. 12 corresponding to $t_0 = 10$ it is impossible for the figure from A_1 to reach the area in the neighbourhood of

n, and the figure from A_2 cannot turn round sufficiently to cover the area at m. The figures from A_2 will therefore cover the area n and the figure from A_1 the area m, as also appears from the Figs. 13, 16 and 18.

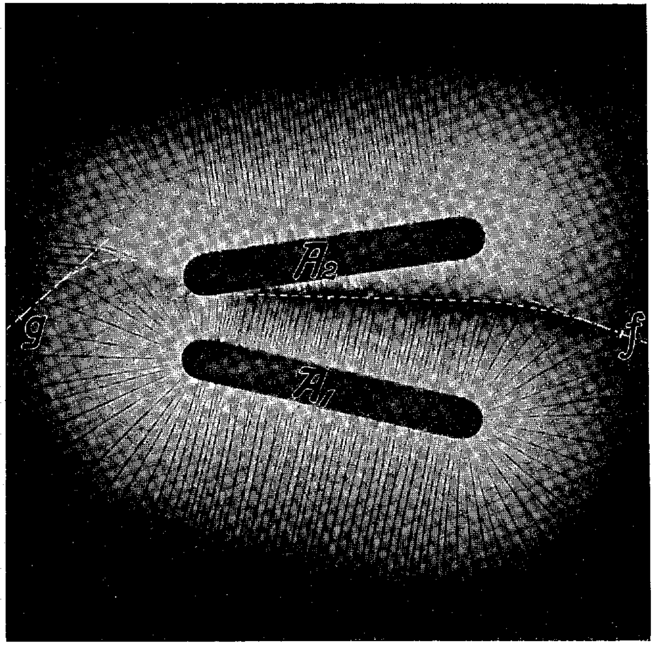

Fig. 13. Negative Velocity Figure. Broken Line shows Theoretical Form of Separating Line.

With negative figures it is impossible to obtain a separating line as that corresponding to $t_0 = 10$ in Fig. 13 without a spark passing between the points B_1 and B_2 on respectively A_1 and A_2. Such a spark may pass so early that it alters the position of the separating line. In velocity or time measurements by means of negative figures it is, therefore, always necessary to place the electrodes A_1 and A_2 at such a distance from each other that the point where the separating line reaches the edge of A_2 is rather close to the point B_2. With positive figures, where the tendency to spark-over is much smaller, the position of A_1 and A_2 is not so critical.[1]

The two end points f and g of the separating line (see Fig. 12) deserve a little consideration. Supposing the ratio of the instantaneous velocities of the two figures is known it is easy to determine the direction of the separating line at these points. In Fig. 14 the line fp is vertical to fo'_1. At the time t the figure from A_1 has travelled the distance $R - \Delta r_1$ and the figure from A_2 the distance $R - \Delta r_2$, where R is the final range. The ratio $\frac{\Delta r_2}{\Delta r_1}$ must, according to the equations, (3) and (5_2), be equal to the constant ratio k of the velocities.

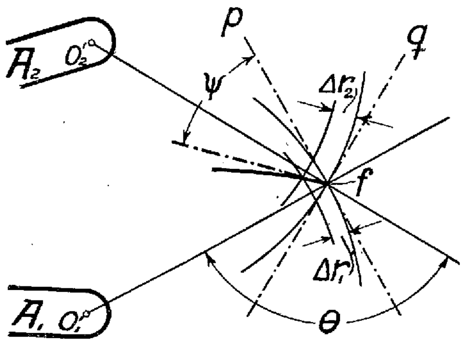

Fig. 14. Direction of the Tangent to the Separating Line in the End Point f.

It is easily shown that the angle ψ between the tangent to the separating line at f and the line fp is determined by

$$\operatorname{tg} \psi = \frac{\sin \theta}{k + \cos \theta}, \tag{12}$$

where θ is the angle between the lines fo'_1 and $o'_2 f$.

If the angles ψ and θ are known, the ratio k is given by

$$k = \frac{\sin \theta}{\operatorname{tg} \psi} - \cos \theta. \tag{13}$$

From equation (12) it follows that

[1] This difference between positive and negative figures will be discussed elsewhere.

for $\quad k = \infty, \quad 1, \quad 0$

we have $\quad \psi = 0, \quad \frac{1}{2}\theta, \quad \theta.$

The correctness of these values is evident.

From equation (8) it follows, that

$$k = e^{\alpha t_0} = \frac{R}{R-a}. \tag{14}$$

That is, the value of the ratio k depends only on the values of R and a.

We have until now supposed that the final ranges R_1 and R_2 of the figures from A_1 and A_2 are equal. Generally that is not the case, R_2 for positive figures being somewhat smaller and for negative figures considerably greater than R_1. Further particulars about this question are to be found in L. F. I p. 32—33 and need not be discussed here. It is sufficient to point out that the position of the point c in Fig. 12 — and therefore the measured value of a — depends solely on the velocity (and range) of the figure from A_1. If, however, $R_1 \neq R_2$, the position of the points f and g are changed and the equations (12) and (13) do not hold good any longer.

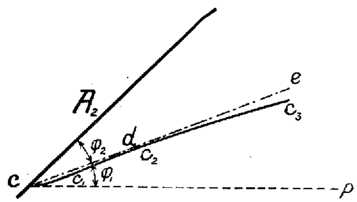

Fig. 15. $e\,c$ Theoretical Separating Line. $c\,c_1\,c_2\,c_3$ Actual Separating Line deformed by the Electric Field from the Charge on A_2 and its Figure.

Even if $R_1 = R_2$, the electrical fields due to the figures themselves will to a certain extent alter the theoretical forms of the separating lines. This deformation is, however, in most cases very small. We shall briefly consider these influences and suppose for the sake of simplicity that the front of the impulse is vertical. The figure from

A_1 (see Fig. 15) has just reached the line cp at the moment the impulse reaches A_2. If then the ratio between the velocity of the two figures is constant, the separating line will be a straight line ce through the point c. The electric field due to the charge on A_2 and on the figure spreading from A_2 will, however, cause some slight deformations of

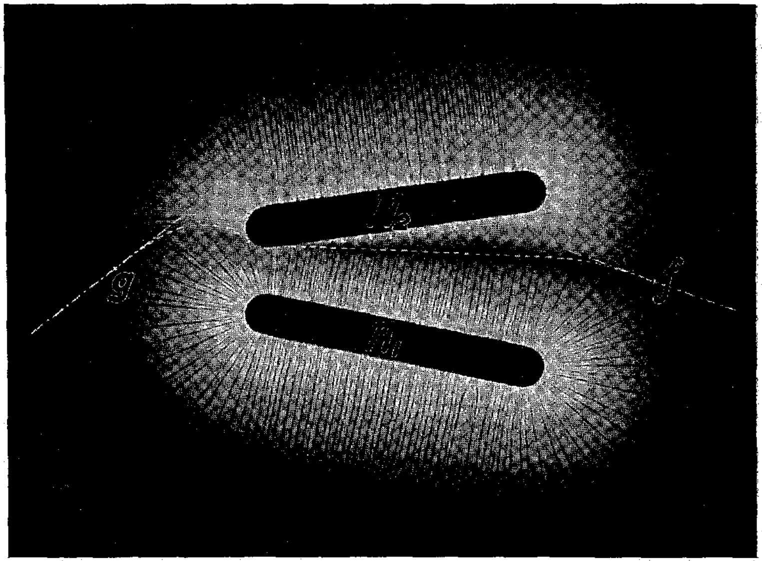

Fig. 16.

this line. The main effect of this field is that it retards the spreading of the figure from A_1 especially between the points c and d. Another, but generally very small effect, is the retardation of the spreading-velocity of the figure from A_1 between the points d and e resulting in a bending down of the separating line as shown in the curve $c_2\, c_3$. This effect is only perceptible if the point e is at a distance from A_1 very nearly equal to the final range of the figure from A_1. In this case the electric density is much greater above than below the separating line and the figure from A_1 will therefore be retarded.

It is mainly in positive figures that the deformation at c_1 appears. This is no doubt, partly at least, due to the fact, that positive figures do not commence to spread be-

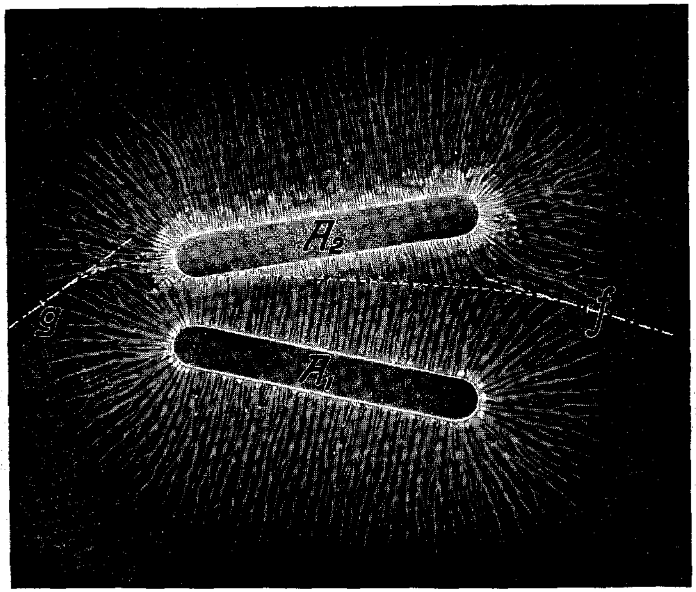

Fig. 17.

fore the tension has attained a certain value dependent upon the condition in the experiment, compare L. F. I p. 51 and 54, and the note on page 32 in the present paper.

Generally speaking the above mentioned deformations of the straight separating line are only very small and the position of the point c may therefore be determined with considerable accuracy. It is a great help in this that the angle φ_2 which the theoretical straight separating line forms with A_2 may be calculated according to equation (10_2).

How closely the theoretical form of the separating line agrees with the actual one will be evident from an inspection of the negative velocity figure in Fig. 16 and the positive ones in Fig. 17 and 18. Furthermore we have on

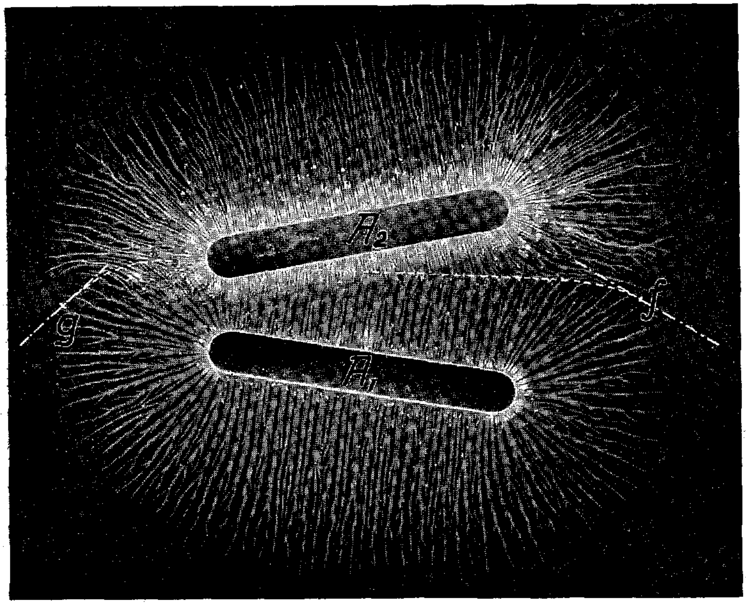

Fig. 18.

Plate 1 and 2 shown some magnifications of the straight part of the separating line from some positive — Plate 1 parts I-IV and Plate 2 Parts I-II — and negative — Plate 2 Parts III-IV — velocity figures. A closer inspection will show the remarkable "straightness" of these parts of the separating line. The bending down of this line close to A_2 in Parts II-IV on Plate 1 is due to a sloping wave front (see Fig. 12) and to the electric field from A_2, compare Fig. 15. The bent part $a\,b$ in part II on Plate 2 is due to the end of A_1.

From an inspection of the figures on Plate 1 and 2 it is evident that the straight part of the separating line may — with the use of a magnifying glass — be drawn with great certainty. When the negative velocity figures in Figs. 13 and 16 give the impression that there is a rather great uncertainty with regard to the position of that line, this is only due to the circumstance that some of the details which serve to fix the exact position of the said line — and which are to be seen in parts III and IV of plate 2 — although very clear in the original plates have been lost in the copies.

As a further verification of the correctness of our results we may compare the angle φ_2 between the electrode A_2 and the straight part of the separating line measured on the plate with the value of that angle calculated according to the equations (10_2) and (11). A long series of measurements have shown that the observed and the calculated values of φ_2 agree fairly well, the differences being within the limits of possible errors. As an example we quote in Table 1 three such sets of measurements.

Table 1. Positive Velocity Figures.

Plate	R	a	φ_0	$\Delta\varphi$	φ_2 cal.	φ_2 obs.	φ_2 cal. — φ_2 obs.
M. 324	30 mm	8.6 mm	22°	3.7°	12.8°	12.5°	+ 0.3°
» 320	31 »	10.9 »	21°	4.5°	12.5°	12.6°	— 0.1°
» 327	34 »	13.0 »	19°	4.5°	11.8°	12.2°	— 0.4°

The two negative velocity figures Figs. 13 and 16 and a third one not reproduced here seem to form an exception to this agreement. The data for these three figures

Table 2. Negative Velocity Figures.

Plate	R	a	φ_0	$\Delta\varphi$	φ_2 cal.	φ_2 obs.	φ_2 cal. — φ_2 obs.
M. 319	32 mm	9.0 mm	21.2°	3.5°	12.3°	10.0°	+ 2.3°
» 320	25 »	9.5 »	19.2°	4.4°	11.8°	10.2°	+ 1.6°
» 321	32 »	12.0 »	20.0°	4.6°	12.3°	10.6°	+ 1.7°

are collected in Table 2, from which it appears that the calculated values are decidedly greater than those observed, and the differences are outside the limit of the possible errors. The cause of this discrepancy is the following:

As mentioned before the final range R_2 is — with relatively great values of t_0 — considerably greater than the range R_1. In order to investigate the correctness of the equations (12)—(14) for negative figures it was necessary to arrange matters in such a way that the two ranges become equal. In order to obtain this equality in range a shunt was inserted between the point c (see Fig. 1) and earth and the resistance of this shunt was given such a value that $R_1 = R_2$. Another effect of this shunt is, however, that the voltage at A_2 becomes somewhat less than the voltage at A_1, and consequently φ_2 obs. must be smaller than the value of φ_2 calculated by means of the equations (10_2) and (11).

In Figs. 13 and 16—18 we have shown the direction of the tangents to the separating line at the points f and g calculated by means of the equations (12)—(14). For the points f the calculated direction of the tangent agrees fairly well with the actual direction of the separating line at these points. For the points g there is no such agreement and the cause hereof is mentioned before and needs no further comment. Still it may be worth while to point out that the lines in the negative figures are straight from the electrode A_1 and right to the theoretical separating line in the neighbourhood of the point g, and that they have a rather sudden bend where they pass over the said line, see especially Fig. 13.

The experiments have thus confirmed all the conclusions which we have drawn from the equations (5_2), (8) and (9).

6. The Measurement of Very Small Intervals of Time. Concluding Remarks.

We are now in such a position that we can use the spreading of the Lichtenberg figures for the determination of a very small interval of time t_0 which passes from the moment one electric impulse reaches the electrode A_1 to the moment when another impulse reaches A_2. In order to do this it is only necessary to determine the corresponding A-curve with a as abscissa and t_0 as ordinate, where a is the distance from the point c to the edge of the electrode A_1, c being the point where the straight part of the separating line cuts on the edge of A_2, see Figs. 3—6 and 12.

In practice there is no difficulty in fixing the position of the straight part of the separating line with sufficient accuracy. It is most easily done in the following way: A preliminary line is drawn and the corresponding value of a measured. With this value of a and the measured value of R_1 the angle φ_2 is calculated from the equations (10_2) and (11). A new straight line forming this angle with A_2 is then drawn in such a position, that it coincides as closely as possible with the actual separating line. In doing this a magnifying glass is of great help. If the new value of a corresponding to this separating line does not differ considerably from the first, the new value of a may be taken as the correct one, if not, the procedure must be repeated once more. With a little experience this repetition will generally be found unnecessary. With the thus determined value of a we take from the A-curve the corresponding value of t_0.

This is, however, only true for those parts of the curves A in Figs. 4—6, which are drawn in full line. There is some uncertainty both for very small values of a and for such values which are but little smaller than the final range R. With regard to the first part there can be no doubt whatever that the wave front is not vertical, and the A- (and B-) curves must therefore necessarily have another form than that corresponding to equation (8) and (9). The first part of the A- and B-curves will, really, have a shape similar to that shown in dotted lines in Fig. 19.

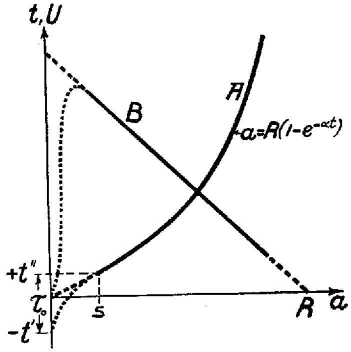

Fig. 19. Probable Form of the A- and B-Curves for Sloping Wave Front and for Very Small Values of a.

The A-curve will start from a point $-t'$ of the t-axis and the B-curve from the origin. The velocity curve will also, as shown in Fig. 20, start from the point $-t'$ of the t-axis. The duration of the sloping wave front is in both figures denoted by τ_0, and the symbols t' and t'' are the same as those used in Fig. 10.

In the Figs. 4—7 t_0 is the time interval between the arrivals of the vertical fronts of the equivalent waves and, as shown before, the irregularities due to the sloping of

Résumé.

It has been shown that the three equations (I)—(III) on page 2 have the following forms:

$$r = R(1 - e^{-\alpha t}), \tag{I'}$$

$$U = \alpha R e^{-\alpha t} = U_0 \cdot e^{-\alpha t}, \tag{II'}$$

and

$$t = \frac{1}{\alpha} \operatorname{lognat} \frac{R}{R - a}. \tag{III'}$$

Some values of the constant α are given in Figs. 8 and 9.

The author desires to express his thanks to Mr. J. P. CHRISTENSEN and Mr. A. G. JENSEN for their valuable assistance during this investigation.

The author also desires to acknowledge his indebtedness to the CARLSBERG FUND for its support of these investigations.

The Royal Technical College, Copenhagen,
Telegraph and Telephone Laboratory.

Bibliography II

containing some papers which were overlooked in the preparation of the first Bibliography or which have appeared since its publication.

RAGNAR ARPI: Synthetische Studien über Dendritenstruktur, auf Metallographie und elektrische Entladungen angewendet. Arkiv f. mat., astr. och fysik. Bd. 8. Nr. 14. 1912.

B. ELL: Ny method att medels ljuskänsligt preparerade papper eller plåtar åskådliggöra kraftlinjernas riktning och relativa antal i ett elektrisk fält. Teknisk Tidskrift. Afd. Elektroteknik. 51. Årg. p. 49—55. 1921.

K. PRZIBRAM: 1. Beiträge zur Kenntniss des verschiedenen Verhaltens der Anode und Kathode bei der elektrischen Entladung. Wien. Ber. Math. naturw. Cl. Bd. C VIII. Abth. II a. p. 1161—1171. 1899.

— 2. Vorläufige Mitteilung über die photographische Aufnahme der elektrischen Entladung auf rotierenden Films. Ibid. Bd. C IX (II a). p. 902—904. 1900.

— 3. Photographische Studien über die elektrische Entladung. Ibid. Bd. C X (II a). p. 960—963. 1901.

— 4. Ueber das Leuchten verdünnter Gase im Teslafeld. Ibid. Bd. C XIII (II a). p. 439—468. 1904.

— 5. Ueber die Büschelentladung. Ibid. Bd. C XIII (II a). p. 1491—1507. 1904.

— 6. Büschel- und oszillierende Spitzenentladung in Helium, Argon und anderen Gasen. Ibid. Bd. C XVI (II a). p. 557—570. 1907.

— 7. Die Büschelentladung in Clor und die Beziehung zwischen Büschelentladung und Jonenbeweglichkeit. Ibid. Bd. CXXI (II a). p. 2163—2168. 1912.

— 8. Einpolige elektrische Figuren und Elektronenaffinität. Ibid. Bd. 127 (II a). p. 395—404. 1918.

— 9. Ueber die elektrischen Figuren. Phys. Zeitschr. 19. p. 299—303. 1918.

— 10. Form und Geschwindigkeit. Die Naturwissenschaften. Heft. 6. p. 103—107. 1920.

— 11. Ueber die Ladung der elektrischen Figuren. Wien. Ber. Math.-naturw. Kl. Abt. II a. 128 Bd. p. 1203—1221. 1919.

K. PRZIBRAM: 12. Ueber die elektrischen Figuren. II. Mitteilung. Phys. Zeitschr. 21. p. 480—484. 1920.

— 13. Der Vorsprung der negativen Entladung vor der positiven. Wien. Ber. Math. naturw. Kl. II a. Bd. 129. p. 151—160. 1920.

K. PRZIBRAM und E. KARA-MICHAILOVA: Orientierte Gleitbüsche auf Kristallflächen. Zeitschr. f. Physik. 2. p. 297—298. 1920.

J. SPIESS: Ueber die auf Wasser gleitenden electrischen Funken. Wied. Ann. 31, p. 975—982. 1887.

A. A. CAMBELL SWINTON: Electrical Discharges. The Electrical Review. Vol. XXXI. p. 273—275. 1892.

M. TOEPLER: Ueber die physikalischen Grundgesetze der in der Isolatorentechnik auftretenden elektrischen Gleiterscheinungen. Archiv für Elektrotechnik. X. p. 157—185. 1921.

USABURO YOSHIDA: 1. Figures produced on Photographic Plates by Electric Discharges. Mem. Coll. Sc. Kyoto Imp. Univ. Vol. II. p. 105—116. 1917.

— 2. Further Investigations on the Figures produced on Photographic Plates by Electric Discharges. Ibid. p. 315—319.

Forelagt paa Mødet den 10. Februar 1922.
Færdig fra Trykkeriet den 20. Juni 1922.

I

+

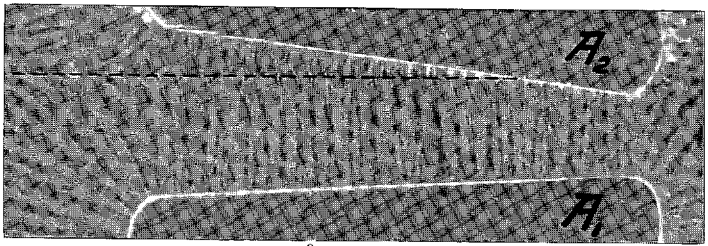

$t_0 = 2.1 \times 10^{-8}$ sec; $p = 300$ mm Hg.

II

+

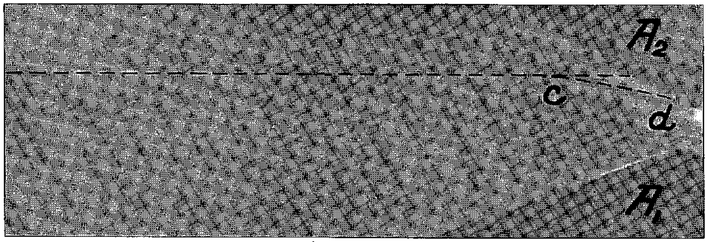

$t_0 = 2.45 \times 10^{-8}$ sec; $p = 150$ mm Hg.

III

+

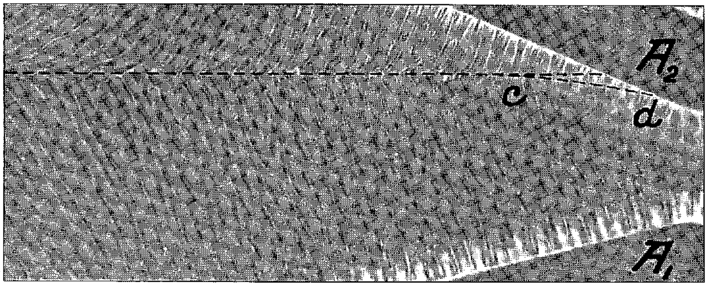

$t_0 = 3.5 \times 10^{-8}$ sec; $p = 500$ mm Hg.

IV

+

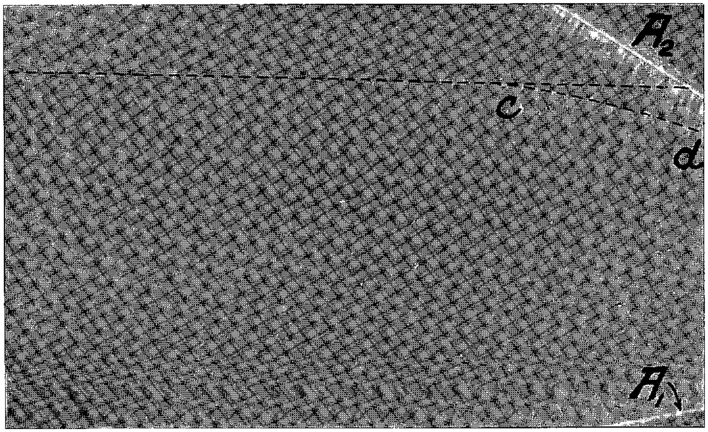

$t_0 = 6.3 \times 10^{-8}$ sec; $p = 300$ mm Hg.

I

+

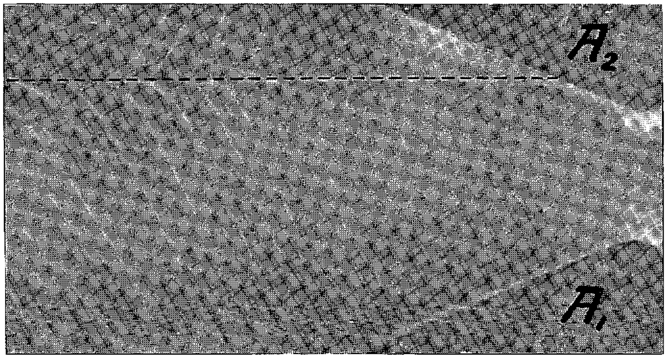

$t_0 = 2.1 \times 10^{-8}$ sec; $p = 150$ mm Hg.

II

+

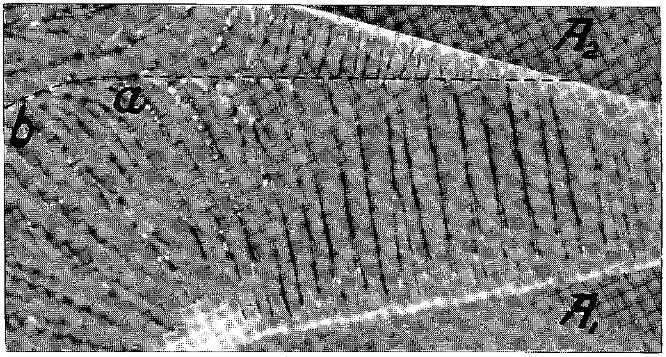

$t_0 = 2.1 \times 10^{-8}$ sec; $p = 300$ mm Hg.

III

—

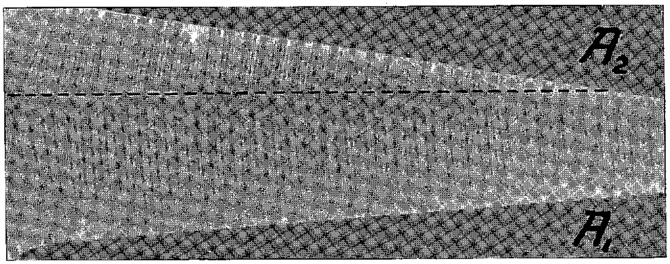

$t_0 = 3.5 \times 10^{-8}$ sec; $p = 400$ mm Hg.

IV

—

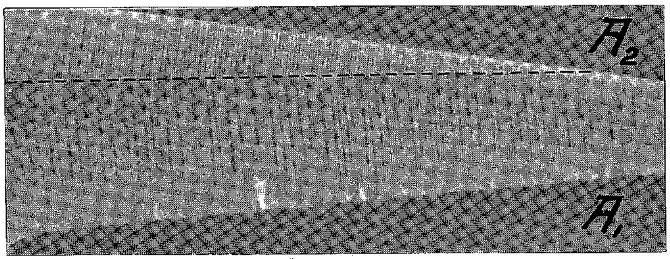

$t_0 = 3.5 \times 10^{-8}$ sec; $p = 400$ mm Hg.